Quarterly Progress Report

N01-NS-1-2333

Restoration of Hand and Arm Function by Functional Neuromuscular Stimulation

Period covered: January 1, 2004 to March 31, 2004

Principal Investigator: Robert F. Kirsch, Ph.D.

Co-Investigators:

Patrick E. Crago, Ph.D.
P. Hunter Peckham, Ph.D.
Warren M. Grill, Ph.D.
J. Thomas Mortimer, Ph.D.
Kevin L. Kilgore, Ph.D.
Michael W. Keith, M.D.
David L. Wilson, Ph.D.
Dawn Taylor, Ph.D.
Joseph M. Mansour, Ph.D.
Jeffrey L. Duerk, Ph.D.
Wyatt S. Newman, Ph.D.
Harry Hoyen, M.D.
John Chae, M.D.
Jonathon S. Lewin, M.D.
Dustin Tyler, Ph.D.

Program Manager: William D. Memberg, M.S.

Case Western Reserve University
Wickenden 407
10900 Euclid Avenue
Cleveland, OH 44106-7207
216-368-3158 (voice)
216-368-4969 (FAX)
rfk3@po.cwru.edu

Contract abstract

The overall goal of this contract is to provide virtually all individuals with a cervical level spinal cord injury, regardless of injury level and extent, with the opportunity to gain additional useful function through the use of FNS and complementary surgical techniques. Specifically, we will expand our applications to include individuals with high tetraplegia (C1-C4), low tetraplegia (C7), and incomplete injuries. We will also extend and enhance the performance provided to the existing C5-C6 group by using improved electrode technology for some muscles and by combining several upper extremity functions into a single neuroprosthesis. The new technologies that we will develop and implement in this proposal are: the use of nerve cuffs for complete activation in high tetraplegia, the use of current steering in nerve cuffs, imaging-based assessment of maximum muscle forces, denervation, and volume activated by electrodes, multiple degree-of-freedom control, the use of dual implants, new neurotization surgeries for the reversal of denervation, new muscle transfer surgeries for high tetraplegia, and an improved forward dynamic model of the shoulder and elbow. During this contract period, all proposed neuroprostheses will come to fruition as clinically deployed and fully evaluated demonstrations.

Summary of activities during this reporting period

The following activities are described in this report:

- *Intraoperative testing of nerve cuff electrodes and implant tools*
- *Wireless data acquisition module for use with a neuroprosthesis.*
- *Adaptive neural network controller for an upper extremity neuroprosthesis*
- *An integrated voluntary muscle and FES controller to restore elbow extension in spinal cord injury*

Intraoperative Testing of Nerve Cuff Electrodes and Implant Tools

Contract sections:
E.1.a.i.4.3 Nerve Cuff Electrode fabrication and implantation

Introduction

The purpose of this section of the contract is to fabricate and develop the surgical methods to implement nerve cuff electrodes in a Functional Electrical Stimulation system. The final steps prior to clinical implementation of the nerve cuff electrodes include development of a tool to facilitate cuff implantation and feasibility testing of both the cuff electrode and the tool. These studies are the final preparation for the implantation of four nerve cuff electrodes with percutaneous leads in an individual with high tetraplegia. This quarter, intraoperative testing was performed on one additional subject and the final implant tool was manufactured.

Tool update

A prototype of the implant tool was professionally fabricated by Miltex, Inc. (Figure 1). The tip separation was larger than specified, so the tool was bent slightly to correct for this. After this modification, the tool was used on a cadaver by a surgeon with no previous experience using either the nerve cuff electrode or the implant tool (Figure 2).

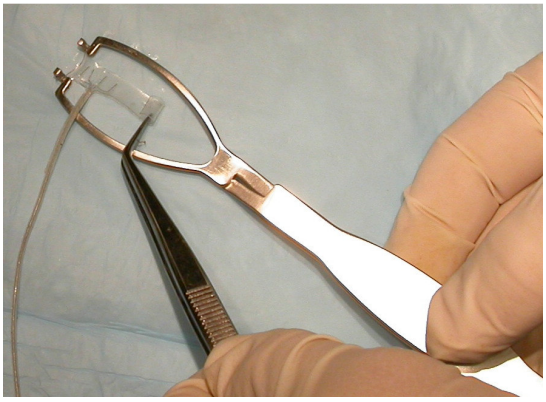

Figure 1. Implant tool with nerve cuff electrode loaded and unrolled.

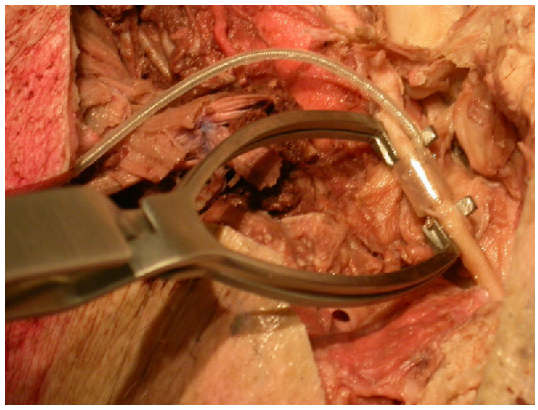

Figure 2. Implant tool after implant of cuff electrode in the neck of a cadaver.

Additional testing of this implant tool will be performed intraoperatively during the next quarter. We are working with Miltex to order additional tools for this and other projects.

Intraoperative testing update

One subject was tested this quarter (Table 1). No motor response was recorded but the SSEP threshold stimulation level was in the range of those previously found.

TABLE I
SUMMARY OF INTRAOPERATIVE TESTING DATA

Subj#	Injury/Condition	Time Post Injury	Threshold***		Stim Pos
			Nerve	Stim Params	
4	Brachial plexus avulsion	9 weeks	Ant. C5	200 μs, 2.0 mA	WC

Legend: WC – whole cuff; Stim Position contains a number that refers to the cuff rotation around the nerve and a letter that refers to the contact on the cuff. ***Threshold values are the lowest recorded value that resulted in a response at the stimulation position indicated.

An intraoperative data collection system has been developed to increase the amount of data collected in the limited amount of time available. The new system includes an automated recruitment curve measurement procedure, which should obtain recruitment curves in 1-2 minutes. This additional data will allow better characterization of the cuff electrodes and provide more detailed selectivity information. This system should be deployed in the next quarter.

Wireless Data Acquisition Module for Use with a Neuroprosthesis

Contract section: E.1.a.v Sensory feedback of contact and grasp force

Abstract

A general wireless data acquisition module (WDAM) is being developed for use with a neuroprosthesis. The WDAM is intended to be used with sensors such as the shoulder or wrist position transducer, finger-mounted joysticks, or remote on-off switches. Currently these sensors are connected to a controller via cables, which are cosmetically unappealing to the user and often get caught on wheelchairs, causing them to be damaged. Switch-activated transmitters mounted on walkers have been used previously in FES applications [1]. Recent advances in wireless technology have reduced the complexity and size of the wireless circuitry and have increased the likelihood that a small, low power, reliable wireless link could be assembled from commercially available components.

Methods

In the previous two quarters, the success of the prototype wireless data acquisition module was demonstrated. Depending on the data transmission protocol, packets were successfully transmitted from 93% to 97% of the time. Power requirements were in the 10 mW range, which was low enough to allow the module to operate off a coin cell battery for up to 74 hours of continuous use.

In this quarter, a printed circuit board (PCB) version of the WDAM was designed and fabricated. The PCB version is a small version of the prototype that allows us to test most of the components that will be used in the user-wearable WDAM, while still allowing some testing of options, such as different types of antennas. This PCB version may also be used as the master wireless module, which collects information from the wireless sensor modules and sends the information via a serial connection to an external controller. The PCB version should reduce the circuit noise level by replacing the soldered wires of the prototype with the printed circuit board traces, which may increase the successful transmission rate. In addition, the PCB version uses surface mount components and a four-layer board that includes a ground plane (just as the user-wearable version will), thus giving a better indication of how the final design will function.

The circuit was designed with Eagle PCB Design software (CadSoft Computer, Inc.). The transceiver, microcontroller, power conditioning, and analog input conditioning sections of the circuit were all placed on a single board. The board layout files were sent to a PCB fabrication company and four boards were made. The surface mount components were assembled at our own facility.

While waiting for the PCB fabrication, an initial layout of the miniature, user-wearable WDAM was done. The user-wearable WDAM is envisioned to be a stack of three circuit boards that are 1 inch squares, producing a 1 inch cube that can be mounted on the hand or arm. In this design, the battery and power conditioning circuitry would go on one board, the transceiver and microcontroller circuitry would go on a second board, and the analog input conditioning circuitry would go on a third board. The initial board layout will be revisited once testing of the PCB version is completed.

Results

The circuit layout and board fabrication process worked well, with the resulting PCB version of the WDAM working according to design. The board is shown in Figure 3.

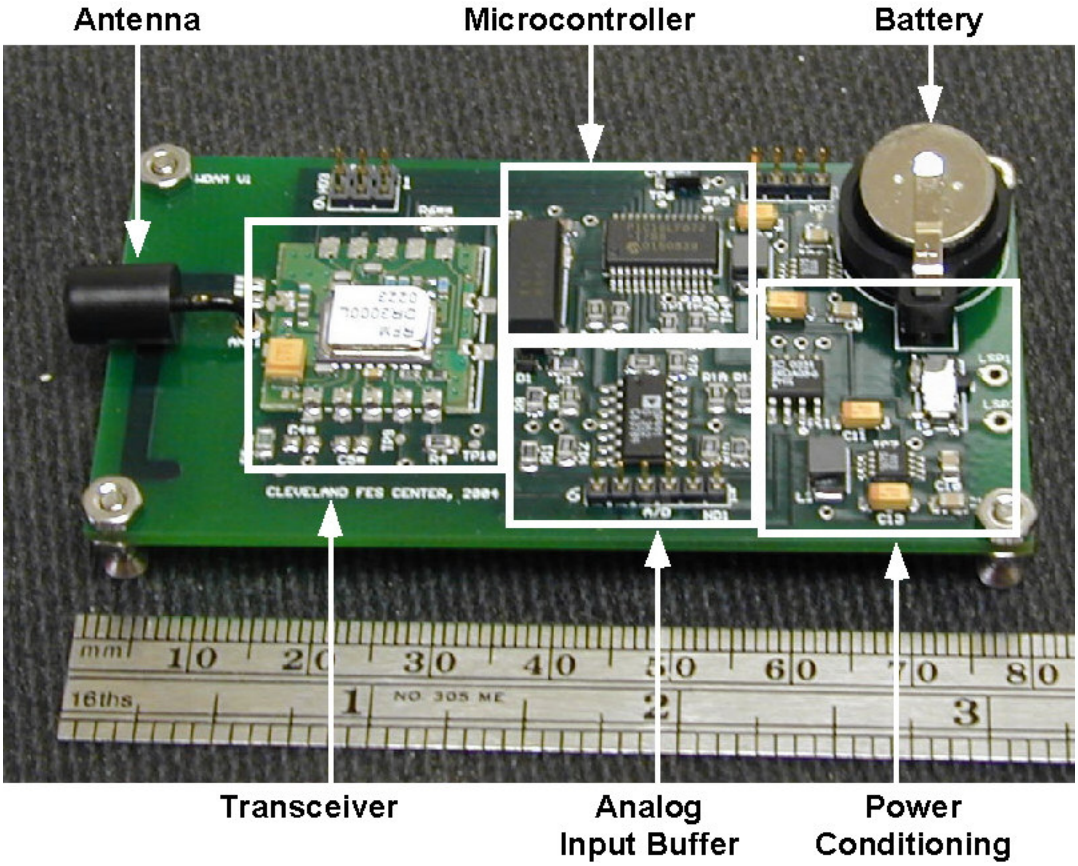

Figure 3. Printed Circuit Board version of Wireless Data Acquisition Module

Testing of the board began at the end of the quarter. An initial test indicated that the PCB version performed slightly better than the previous, larger prototype version. Of 1000 data packets that were sent, 998 were successfully received and acknowledged, although half of them needed to be sent more than once before they were accepted. More tests are being performed to further evaluate this board.

The initial layout of the user-wearable WDAM is shown in Figure 4. Although the boards currently are slightly larger than 1 inch square, this size should be able to be reduced by optimizing the layout and by utilizing smaller components, which are available but would require fabrication by an outside facility with the appropriate equipment.

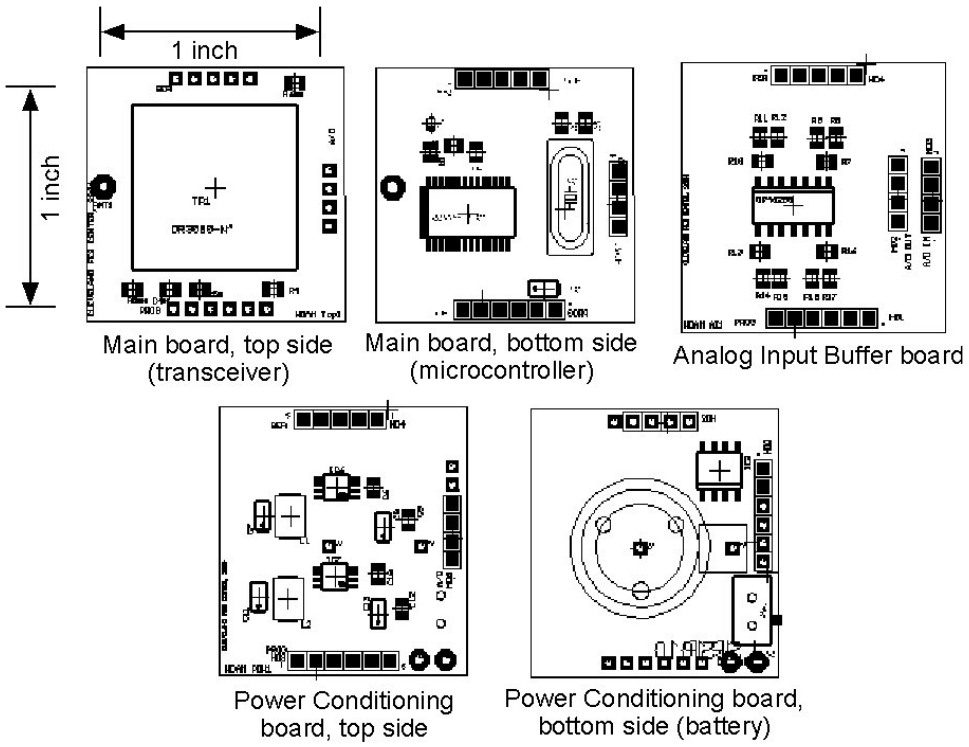

Figure 4. Initial layout of user-wearable WDAM, consisting of 3 stacked boards.

Next Quarter

In the next quarter, the PCB version of the WDAM will be evaluated further. This will include testing of different antenna types. In addition, faster transceiver modules will be placed on the PCB version and evaluated. The fastest transceiver module has a data rate that is 50 times faster than the one currently in use. Although we do not anticipate needing data transmission rates that are that high, the quicker rates will allow the transceiver to spend more time in sleep mode, and therefore will reduce the power requirement further.

References

[1] Z. Matjacic, M. Munih, T. Bajd, A. Kralj, H. Benko, and P. Obreza, "Wireless control of functional electrical stimulation systems," *Artif Organs*, vol. 21, pp. 197-200, 1997.

Adaptive Neural Network Controller for an Upper Extremity Neuroprosthesis

Contract Section: E.2.a.ii.4.1 EMG-based shoulder and elbow controller

Abstract

The long term goal of this project is to develop an adaptive neural network controller for an upper extremity neuroprosthesis targeted for people with C5/C6 Spinal Cord Injury (SCI). The challenge is to determine how to simultaneously stimulate different paralyzed muscles based

on the EMG activity of muscles under retained voluntary control. The controller will extract the movement intention from the recorded EMG signals and generate the appropriate stimulation levels to activate the paralyzed muscles. To test the feasibility of this controller, different arm movements were recorded from able-bodied subjects. Using a musculoskeletal model of the arm, modified to reflect C5/C6 SCI, inverse simulations provided muscle activation patterns corresponding to these movements. Activation patterns were used to train a time-delayed neural network to predict paralyzed muscle activations from voluntary muscle activations.

Introduction

Individuals with C5/C6 SCI lose control over a number of muscles in their upper extremity. Specifically their hand muscles are paralyzed; there is partial loss of wrist and elbow extension; and several shoulder functions are lost, including horizontal flexion and adduction. Arm movements are a coordinated action of several muscles acting upon different joints resulting in a large workspace and fine positioning control. Paralysis of some these muscles lead to a considerable reduction in the reachable workspace. Functional Electrical Stimulation (FES) can be used to stimulate paralyzed muscles whose innervations remain intact, restoring function in individuals with SCI. However, determining the timing and intensity required for simultaneously stimulating different paralyzed muscles in the arm is still a big challenge.

The long term goal of this project is to determine which, how and when to stimulate each of the available muscles in a coordinated fashion to increase the arm's workspace and thus provide a functional benefit to the paralyzed individual. The proposed approach exploits retained voluntary function by extracting the movement intention from the EMG activity of muscles that are under voluntary control and using this information to determine the levels of stimulation required. Based on this principle, positioning and stability in the limb become a synergistic action between the remaining nervous system and the adaptive mechanism of the artificial controller.

Previous work in our lab has shown that an approach of this kind is feasible. Au et al. demonstrated that a neural network is capable of predicting shoulder and elbow joint angles using EMG signals from selected muscles. Parikh et al. used a musculoskeletal model of the arm to obtain the muscle activations required to hold the arm in a certain posture and then used a neural network to predict paralyzed muscle activations using voluntary muscle activations as inputs. Finally, Giuffrida used a neural network to predict triceps stimulation levels for elbow extension using the EMG activity from the biceps muscle as the input. This work gives strong evidence that EMG signals are useful to predict movement intention and generate adequate stimulation patterns.

The goal of the work presented here was to demonstrate the feasibility of controlling a neuroprosthesis using retained voluntary function. The next step is to design a controller to simultaneously restore multiple arm functions. It will include the dynamic characteristics of the arm by recording and utilizing muscle activation patterns from movements instead of static positions. Artificial intelligence and adaptive control techniques are being used to design the controller. The data to train it is obtained from simulations generated by a musculoskeletal model of the arm.

Methods

Experiments to record arm movements in able-bodied subjects were conducted to obtain kinematic data. This data was the input to a musculoskeletal model of the shoulder and elbow.

The model was modified to reflect a C5/C6 SCI individual. After running inverse dynamic simulations, the model provided muscle activation patterns corresponding to the movements recorded. Muscle activations were divided into voluntary and paralyzed muscles (denervated muscles were removed as they cannot be used for stimulation or recording). An artificial neural network (ANN) was trained to predict paralyzed activations using the voluntary activations as inputs. The next step included running forward simulations to obtain predicted movements and used the kinematic errors to drive an adaptive controller that accounted for disturbances in the system. Figure 5 summarizes the strategy described here.

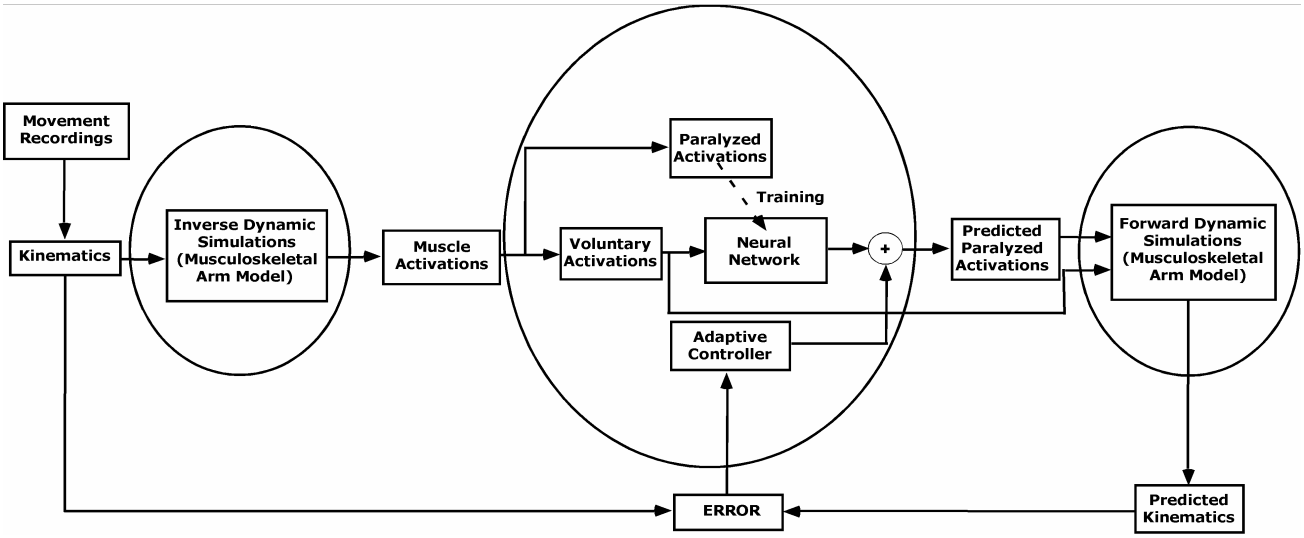

Figure 5. Controller design approach using musculoskeletal modeling.

Arm movements from able-bodied subjects were recorded using an Optotrak system (Northern Digital Inc.) that consists of three infrared cameras capable of recording the 3D positions of light emitting diodes (LEDs) located within the workspace. Sets of LED clusters were fixed over the thorax, upper arm and forearm of the subject. The locations of the scapula and clavicle were difficult to track dynamically, so a scapular palpator with a fourth cluster of LEDs was used to track the position of the scapula during static trials in different positions within the workspace [Veeger, et. al. 2003]. This data and the dynamical orientation of the humerus were used to recover the orientation of the scapula and the clavicle by regression that represents a standard shoulder rhythm [De Groot and Brand, 2001]. Specific bony landmarks were recovered during the movements in order to generate coordinate systems and obtain orientations for each joint in the shoulder and elbow. The recording and data processing were done following the International Shoulder Group recommendations for shoulder and elbow recordings [Van der Helm, 1997]. Figure 6 shows the experimental setup. The movements performed included both single joint movements (shoulder abduction/adduction, flexion/extension, horizontal flexion/extension, internal/external rotation and elbow flexion/extension and pronation/supination), and a set of functional movements comprised of activities of daily living (ADL) such as feeding, drinking, combing the hair, etc. Data was recorded at 50 Hz.

Inverse dynamic simulations were run with the model to obtain muscle activation patterns for the recorded movements. Simulations were done using a musculoskeletal model of the shoulder and elbow developed at the Delft University of Technology [Van der Helm, 1994]. The model was modified to reflect the conditions of a C5/C6 SCI subject by decreasing the maximum forces that could be generated by voluntary muscles with partial paralysis and giving half strength to muscles potentially capable of being stimulated with an FES implant. The mathematical model consisted of finite element descriptions of the bones of the arm (thorax, clavicle, and scapula, humerus, radius and ulna), 28 muscles (some of them divided into various independent elements), four ligaments and 11 degrees of freedom divided in five joints.

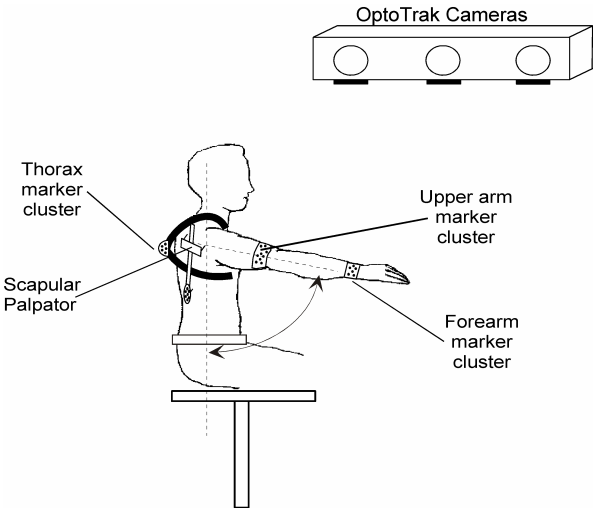

Figure 6. Experimental Setup

A time-delayed artificial neural network (TDANN) was chosen as the basic architecture to predict paralyzed muscle activations (targets) from voluntary muscle activations (inputs). The network had two layers formed by neurons with a tangent-sigmoidal activation function for the hidden layer and a linear activation function for the output layer. Time-delayed inputs were included to be able to capture the spatio-temporal properties of the muscle activations, providing information about the dynamics of the system. The performance of all the networks was measured as its ability to predict data that was not used during the training (the so called generalization ability). This is a highly desirable feature of the controller, because it has to be capable of assisting movements in many different conditions and locations, not just in the ones used during training. To address this issue, the training was done using a bayesian regularization algorithm. This was chosen because it improved the generalization capacity of the network and also gave a measure of how many network parameters are being used effectively by the network, which is helpful in determining the optimal parameters for the TDANN [Demuth and Beale, 2002]. Parameters such as the number of hidden neurons or the number of delays have not been optimized yet, but for these simulations 5 neurons and 5 time delays were chosen based on previous work. The data was split into training, validation and testing data sets. Validation is used during the training to monitor the error generated by the data not used for training. When this error increases, the TDANN is memorizing the training data set and the network is losing its ability to generalize. The testing data set is used to evaluate the performance of the TDANN after the training is finished. The goodness of fit of the TDANN was measured as the RMS error between the predicted and model generated muscle activations. All TDANNs were trained using MATLAB's Neural Network Toolbox (The Math Works, Inc.).

Results

Figure 7 shows a typical kinematic data set obtained after processing the movements recorded. Each plot corresponds to the orientation of each bone segment in the upper extremity

(trunk, clavicle, scapula, humerus and elbow). Each angle corresponds to an Euler angle rotation assigned to represent the orientation of that bone segment according to the standard described in [Van der Helm, 1997]. This data corresponds to one of the ADL tasks performed for 15 seconds.

Once inverse simulations were run, muscle activation patterns were obtained for all the muscles included in the simulation. A subset of muscles was considered to be voluntarily controlled (input) muscles and another set was considered to be paralyzed (target) muscles. Choosing the appropriate muscles and number of muscles is ongoing work. The set of muscles presented here correspond to what are considered candidate muscles for recording and stimulating in a real application. Figure 8 shows a typical set of muscle activations for these two muscle sets corresponding to the movement recordings shown in Figure 7. The top plot shows the muscle activations for the Upper Trapezius, Anterior Deltoid, Infraspinatus and short head of the Biceps, chosen as inputs for the TDANN and potential sources for EMG signal recordings. The bottom plot shows the muscle activations for the Triceps lateral head, Posterior Deltoid, Serratus Anterior and Pectoralis Major, chosen as targets for the TDANN and potential muscles to be stimulated with an FES system.

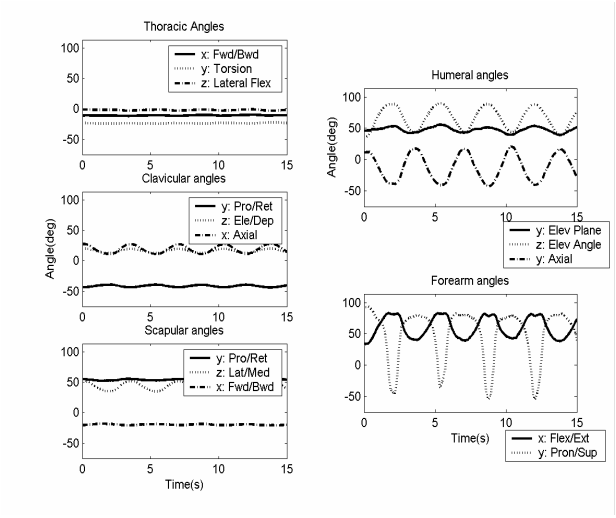

Figure 7. Kinematic data obtained from the movements recorded.

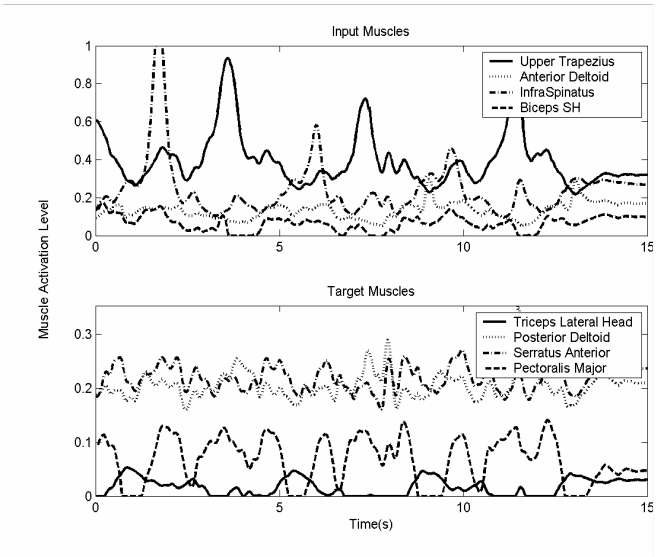

Figure 8. Muscle Activations for TDANN training

Figure 9 shows the predictions of the TDANN for each muscle selected as a target. Solid lines show the target muscle activations and dotted lines show the TDANN predictions. Notice how the prediction captures the main characteristic of the simulated activations. The average RMS error for this data set was 0.0264.

Discussion

The goal of this study is the design of a controller capable of using retained voluntary function to extract the movement intention and generate the appropriate levels of stimulation for paralyzed muscles in people with C5/C6 SCI. After recording movements during experiments with able-bodied subjects and obtaining muscle activation patterns from inverse dynamic simulations with a musculoskeletal model of the arm, an artificial neural network was successfully trained to predict paralyzed muscle activations using voluntary muscle activations as inputs.

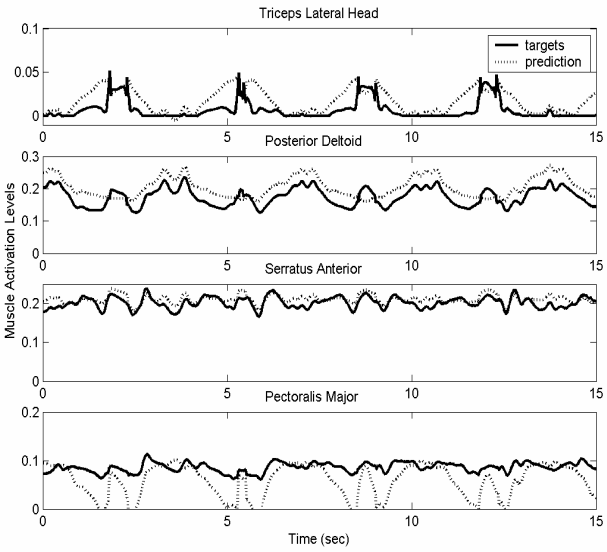

Figure 9. TDANN predictions.

These preliminary findings demonstrated that a TDANN is an acceptable open-loop block for the proposed controller. It was capable of predicting muscle activations with a good accuracy. EMG signals are representative of muscle activations levels; therefore, this approach can be implemented in humans by using signals directly recorded from voluntarily controlled muscles. Errors are anticipated using an open loop strategy, as it does not account for changes in the arm properties during different activities and conditions (e.g. fatigue). An adaptive controller that accounts for these disturbances is proposed as a feedback block for the controller. Present work is focused on evaluating the quality of the prediction and using a feedback error signal to drive the adaptive block. For the work presented here, this will be done by performing forward simulations and using the error between the predicted and the recorded kinematics to drive this block. In a human implementation, sensors that register the arm position or some other means to measure the quality of the movement will be required.

Incorporating retained voluntary control mechanisms exploits the immense adaptive ability of the human nervous system. The hypothesis of this work is that intact portions of the nervous system can re-adapt to the use of the neuroprosthesis and learn to interact with it. The proposed controller will successfully interact with the remaining motor function in a continuous adaptation process, creating a synergistic relation between the nervous system and the neuroprosthesis that will restore function in a natural manner.

Next Quarter

In the next set of inverse dynamic simulations, the optimization criteria will be varied to reflect different nervous system motor control strategies. Then, using the forward dynamic musculoskeletal model developed as part of this contract (section E.1.a.ii..4.3), forward simulations will be performed on the activation patterns predicted by the neural network. The resulting movements will be compared to the experimental movements and the kinematic errors will be used to design an adaptive strategy.

References

Au A., Kirsch R.F. “EMG-Based prediction of shoulder and elbow kinematics in able-bodied and spinal cord injured individuals”. IEEE Transactions on Rehabilitation Engineering. Vol 8, No 4. Dec 2000.

De Groot, J.H., Brand, R. “A three-dimensional regression model of the shoulder rhythm” Clinical Biomechanics. Vol. 16 (2001) 735-743.

Demuth H., Beale M., MATLAB Neural Network Toolbox Vol. 2. The Math Works Inc. Jul 2002

Guiffrida J.P, "Synergistic neural network control of FES elbow extension after SCI using EMG". Ph.D. Thesis. Biomedical Engineering. Case Western Reserve University. Mar 2004.

Parikh P.P., Acosta A.M., Kirsch R.F., "Voluntary synergistic control of shoulder muscle functional neuromuscular stimulation patterns in C5 tetraplegia". Case Western Reserve University. Unpublished.

Van der Helm, F.C.T. "A finite element musculoskeletal model of the shoulder mechanism". Journal of Biomechanics. Vol 27. No 5. pp 551-569. 1994.

Van der Helm, F.C.T. "A standardized protocol for motion recordings of the shoulder". Proceedings of the First Conference of the International Shoulder Group. 1997.

Van der Helm, F.C.T. et al. "ISB recommendation on definitions of joint co-ordinate system of various joints for the reporting of human motion: Pt II. Shoulder and Elbow. Journal of Biomechanics. In press.

Veeger,H.E.J., van der Helm, F.C.T., Chadwick, E.KJ., Magermans, D. "Toward standardized procedures for recording and describing 3-D shoulder movements". Behavior Research Methods Instruments & Computers. 35 (3). Pp 440-446. 2003.

An Integrated Voluntary Muscle and FES Controller to Restore Elbow Extension in Spinal Cord Injury

Contract section: E.2.a.ii.4.1 EMG-based shoulder and elbow controller

Introduction

Individuals with a C5/C6 SCI have paralyzed elbow extensors, yet retain weak to strong voluntary control of elbow flexion and some shoulder movements. They lack elbow extension, which is critical during activities of daily living. Restoring elbow extension should improve quality of life, increase societal participation, and lead to greater independence. Our previous methods to restore elbow extension included constant level FES and reciprocal control. The objective of this research was to develop and assess a synergistic controller using voluntary elbow flexor and shoulder EMG to control stimulated elbow extension. The control system utilized natural synergies, integrating remaining voluntary control with triceps FES. The subject should simply attempt to move their hand to a location or apply an endpoint force and the controller should apply an appropriate level of triceps stimulation (Figure 10). We hypothesized that EMG from remaining voluntarily controlled upper extremity muscles could be used to train a neural network controller to output an appropriate level of triceps stimulation. Additionally, once trained the synergistic network controller should provide functional benefits compared to previous control methods.

Methodology

A. Overview

Four subjects with complete C5/C6 spinal cord injuries participated. All were previously implanted with an FES hand grasp system including an electrode implanted in the paralyzed triceps. A few to several proximal arm muscles were under voluntary control including elbow flexor and shoulder muscles.

The controller should allow subjects to generate and control endpoint force vectors unachievable without triceps stimulation. Achieving forces outside their voluntary range requires triceps stimulation. Additionally, once trained, the network will operate during triceps stimulation. These requirements created a catch-22. An ANN that needed training to output an appropriate level of triceps stimulation needed to be trained with EMG collected during the appropriate level of triceps stimulation. Therefore, a reasonable stimulation level estimate for each goal vector to be attempted during data collection was needed.

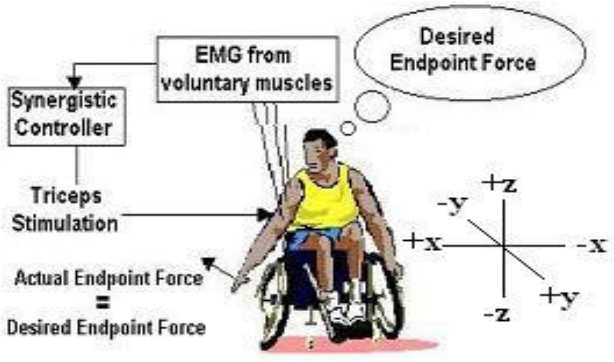

Figure 10. The controller should let a SCI subject move their arm or apply an endpoint force simply by attempting to do so.

B. Triceps Stimulation Level Estimates

A biomechanical model predicted elbow extension moments required by triceps for a specific subject and goal isometric endpoint force vector that the subject would encounter during data collection. We tailored the model to give us subject-specific outputs based on their remaining voluntary muscle set. A value of 1 indicated a normal, voluntarily controlled muscle while 0 represented a completely paralyzed muscle. Weakened muscles were assigned intermediate values depending upon their manual muscle test scores. By defining triceps as near normal, we obtained the triceps elbow extension moment needed to achieve the desired endpoint force.

Elbow moments were converted to stimulation levels by experimentally measuring elbow moment as a function of stimulus level (recruitment curve) using an elbow moment transducer. The stimulation pulse width was increased from 0 μs to 200 μs in steps of 20 μs. A polynomial was fit to scatter plots of elbow extension moment versus stimulation pulse width. The elbow extension moments predicted by the model were then fit to the recruitment curve to estimate required triceps stimulation.

C. Data Collection and Signal Processing

Surface EMG was collected from a subset of C5/C6 SCI subjects' voluntarily controlled muscles while they attempted to match goal isometric endpoint force vectors at a high, mid, and low endpoint location. EMG was recorded from upper, middle, and lower trapezius (UT, MT, LT), anterior, middle, posterior deltoid (AD, MD, PD), biceps (BI), and brachioradialis (BR).

Subjects donned a small cast to stabilize their wrist joint. A visual 3-D display provided force magnitude and direction feedback. Subjects produced discrete goal force vectors in 10 N increments along each axis (Figure 10). Stimulation was delivered to the triceps at 20 mA, 12 Hz, with a variable pulse width based on the model predictions for the particular goal endpoint force. EMG was sampled at 2500 Hz. Blanking amplifiers removed stimulus artifact. Software calculated the RMS value of the EMG segment between each stimulating pulse, normalized it, and filtered it with an adaptive, step-size filter.

D. Neural Network Training and Verification

The EMG signals (inputs) and triceps stimulation levels (outputs) used during data collection were used to train ANN's. MATLAB was used to train a static two-layer structure using one hidden layer with five neurons and an output layer with "tansig" transfer functions at each hidden layer node. Inputs included the voluntary EMG command signals, and the output was the triceps stimulation level used to obtain the goal force vector. We trained the ANN structure using every possible combination of input muscle sets (i.e. 255 combinations for 8 muscle inputs).

The best set of muscles for a particular subject controller was selected on the basis of 1) reducing the mean squared error (MSE), 2) minimizing the number of required inputs, and 3) operating as predicted by the biomechanical model. First, we verified an acceptable MSE each time a network was trained, both with the training set and with the generalization set. Muscle sets were then selected that minimized the number of required inputs. Next, we qualitatively evaluated whether the trained network controller operated as predicted by the biomechanical model. The discrete time EMG data recorded during tracking of isometric forces along an axis during data collection were used to simulate the trained network operating in real-time. Using those EMG inputs to the trained ANN, we calculated and filtered the controller output (triceps stimulation). The plots of recorded subject endpoint force and simulated controller stimulation output were qualitatively examined to determine if stimulation properly increased or decreased in response to an increase in force in a particular direction (Figure 11, left).

Post-experimentally, the force-stimulation relationship was also examined quantitatively by comparing the relationship predicted by the model to that produced by the trained network. Scatter plots of force versus stimulation were created from the controller simulation plots described above and a polynomial was fit to the scatter points (Figure 11, right). A polynomial was also fit to the force versus stimulation data points predicted by the biomechanical model for the same endpoint location and force axis. The RMS error was computed between the two fitted curves to quantify how well the trained network controller learned the relationship predicted by the model.

E. Real-Time Functional Evaluations

One subject was evaluated for the range of forces they could generate using different control methods. The subject generated maximum forces using three-dimensional visual feedback in each of six randomized directions (Figure 10). Control methods included synergistic control, constant stimulation (200 μs pulse width), and no stimulation (0 μs pulse width). During synergistic control, the stimulation pulse width was a function of the subject's trained ANN controller. A total of nine trials were completed at each endpoint location: three using constant stimulation, three using no stimulation, and three using synergistic control.

The same subject tracked discrete goal forces within his maximum force range at location "mid". One discrete force tracking trial consisted of tracking discrete and slowly ramping isometric force vectors along a single axis. The subject completed twelve discrete isometric force tracking trials. Four trials were completed over each axis, two using constant stimulation (200 μs pulse width) and two using the synergistic controller. The average stimulation pulse width output by the synergistic controller over discrete force intervals along an axis was calculated.

Finally, the same subject was evaluated for functional overhead reach. The task goal was to begin with the hand placed in the subject's lap, obtain a mug on an overhead shelf, bring it

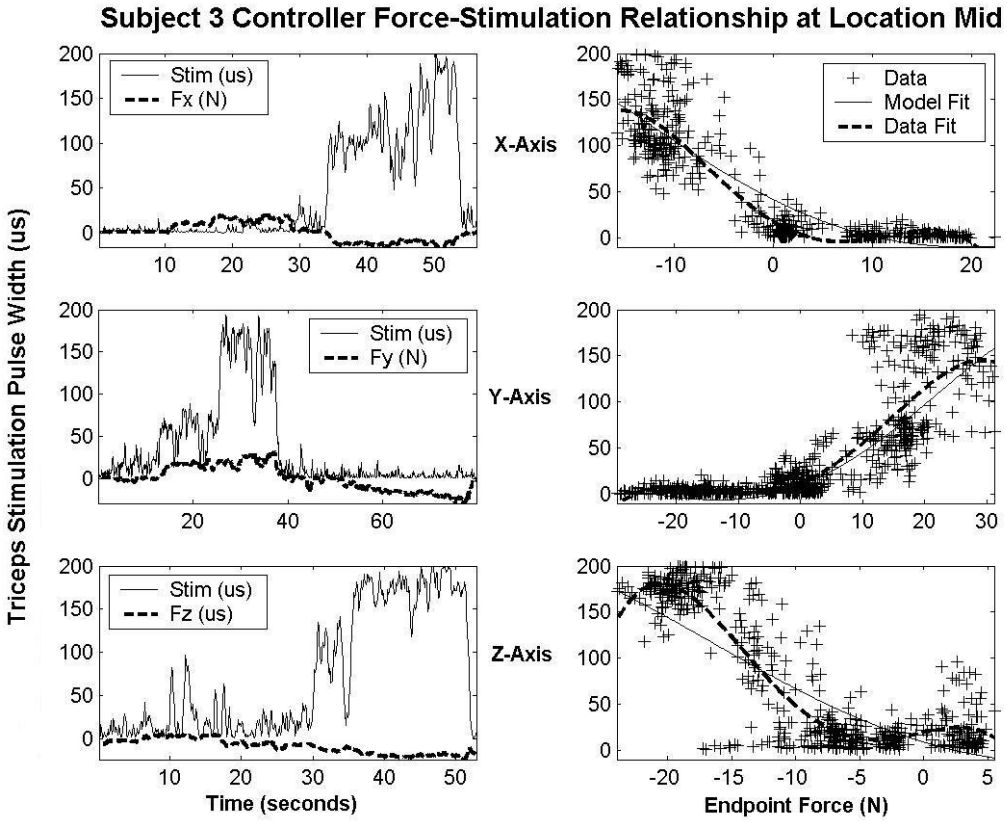

Figure 11. Left column figures are continuous time plots of the force a subject generated along the tracking axis and the stimulation output of the trained network controller using the corresponding EMG from that trial. Right column figures are the data from the corresponding left column figure as scatter plots and a curve fit to endpoint force versus stimulation. Additionally, a curve was fit to the endpoint force versus stimulation data predicted by the biomechanical model.

down to his lap, set the mug back on the shelf, and return his hand to his lap. A total of fifteen trials were completed: five constant stimulation, five no stimulation, and five synergistic controller trials. The time it took to complete a trial as well as a pass/fail assessment of the trial was recorded. A successful trial was recorded when the subject successfully completed all phases of the task.

Results

A. Muscle Selection and ANN Training Verification

ANN's were successfully trained to control triceps stimulation using EMG inputs from proximal arm muscles for all four C5/C6 SCI subjects. An important part of this research was selecting which muscles should be used as inputs to a particular ANN controller. Based on three criteria, only one muscle set out of 255 possible muscle combinations was selected as suitable controller inputs for each subject and/or endpoint location (Table 2). First, trained controllers were eliminated that did not achieve an acceptable MSE. Next, remaining muscle sets were selected that minimized the number of inputs. Thirdly, those controllers were simulated with collected EMG's and the stimulation output was qualitatively compared to the stimulation vs.

force relationships produced by the biomechanical model. The muscle set was selected that qualitatively best fit model results for all force directions.

Subject	Location High	RMS Error (Train, Gen)	Location Mid	RMS Error (Train, Gen)	Location Low	RMS Error (Train, Gen)
1	N/A	N/A	MT, AD, MD	0.035 0.028	N/A	N/A
2	MT, AD, PD	0.117 0.126	MT, AD, BR	0.055 0.050	MT, PD, BR	0.073 0.065
3*	UT, PD, BI	0.020 0.021	UT, PD, BI	0.020 0.021	UT, PD, BI	0.020 0.021
4*	MT,AD,MD,BI	0.024 0.021	MT,AD,MD,BI	0.024 0.021	MT,AD,MD,BI	0.024 0.021

Table 2. Each subject had a particular muscle set used for a particular controller. *One neural network was successfully trained with data from all locations using one muscle set.

For all subjects, increasing the number of EMG inputs reduced the MSE when training or generalization sets were applied to the trained network. Many different muscle sets produced acceptable MSE values. The next criterion was to select muscle sets with the fewest number of muscle inputs. Trained controllers for each subject that passed the first two criteria were then simulated offline. This qualitative evaluation revealed if a trained network properly learned the model predicted relationship between endpoint force and triceps stimulation. Figure 11 illustrates controller simulations using muscle set [UT, PD, BI] for subject 3 at location "mid". As predicted by the biomechanical model, stimulation increased as force increased in the –x, +y, and -z directions and turned off in opposite directions. A single muscle input set was selected for each subject and/or endpoint location that best fit the model relationship predictions. Selected muscle input sets for all subjects and endpoint locations correctly increased or decreased stimulation in 90% (54/60) of force directions.

Post-experimentally, a quantitative analysis computed the RMS error between the model predicted force-stimulation curve fit and the curve fit to the relationship produced by the trained controller (Figure 11). For all subjects and endpoint locations, less than 20% error was observed for 66% (39/59) of force directions.

B. Real-Time Functional Evaluations

In general, for endpoint force directions predicted to require triceps stimulation, the synergistic controller produced larger forces compared to no stimulation. For other directions, where stimulation would interfere with force production, synergistic control produced larger forces compared to constant FES. The full range of endpoint force vectors produced by synergistic control was significantly larger ($p = 0.0006$) than either constant or no stimulation.

The subject could maintain intermediate forces with tracking errors that were not significantly different from those achieved with constant stimulation ($p=0.5956$). A gradient of stimulation was achieved at intermediate endpoint force values (Figure 12). As predicted by the model used to develop the synergistic controller, the average triceps stimulation pulse width increased as the subject generated endpoint forces in the – x, +y, and –z directions. The subject tracked isometric force vectors equally well with each control method, but used 35, 20, and 36% less stimulation over the x, y, and z-axes respectively with synergistic control compared to constant stimulation.

The synergistic controller integrated remaining voluntary function with triceps stimulation during overhead reach (Figure 13). Stimulation increased as the subject's hand approached the mug near when active elbow extension was required. The stimulation decreased as he brought the mug back to his lap. The subject successfully completed all overhead reach

trials using either constant stimulation or the synergistic controller, but failed to complete any trial using no stimulation. However, the subject took significantly longer to complete trials using the synergistic controller compared to constant stimulation (24.6 vs. 12.2s).

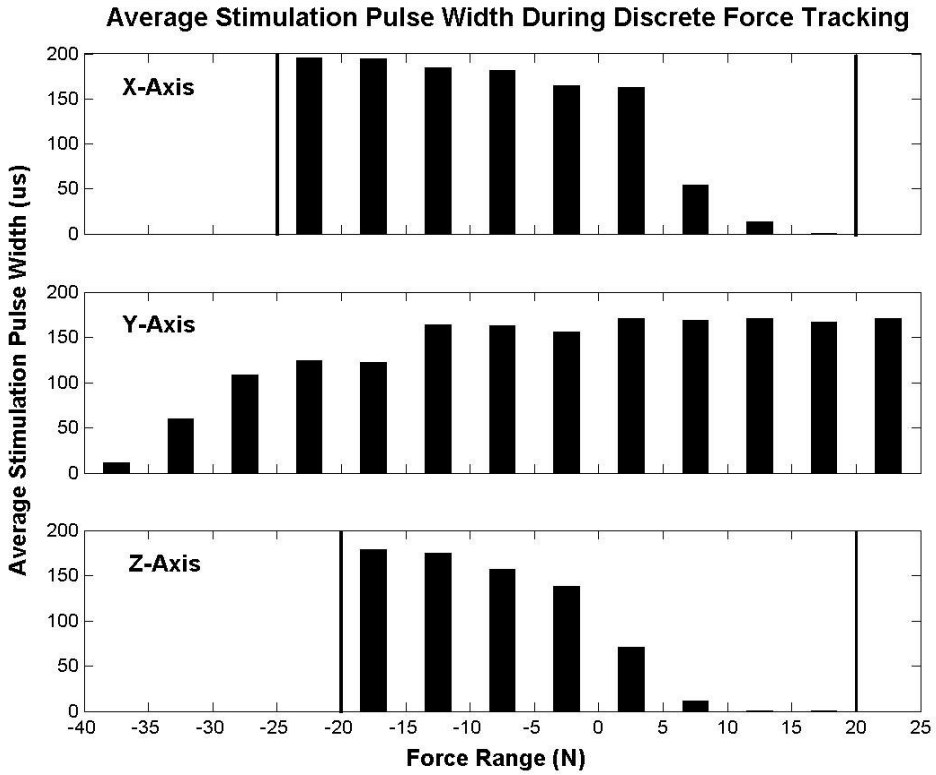

Figure 12. The average stimulation pulse width when the subject's endpoint force was between discrete force ranges is illustrated. Vertical bars illustrate the maximum force the subject generated during tracking.

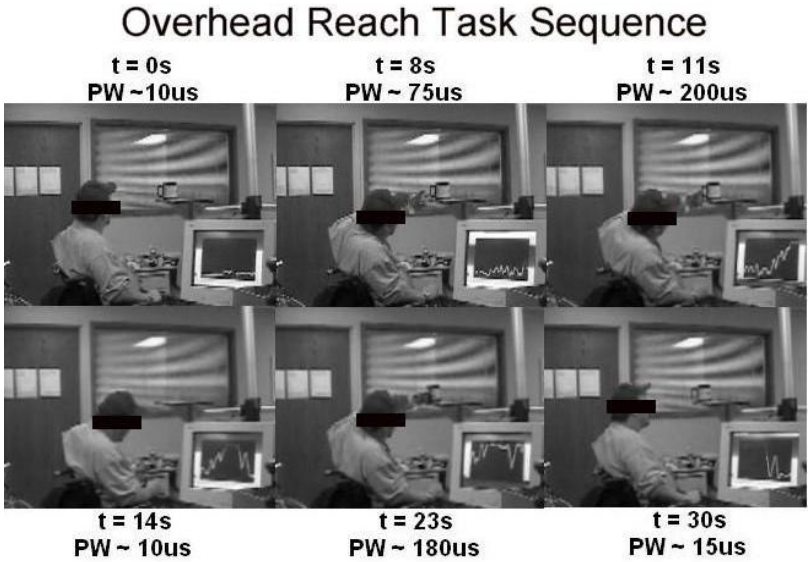

Figure 13. An overhead reach task was completed using the synergistic controller. Shown are six frames of video from a trial. The white trace on the computer monitor illustrates triceps stimulation. The time and stimulation pulse width are shown.

Discussion / Future Work

A set of 3 or 4 muscles, selected for each subject, provided sufficient information to a neural network controller that it produced an acceptable error and effectively learned the relationships between endpoint force and required triceps stimulation as predicted by a biomechanical model. The model derived stimulation estimates enabled us to solve the problem of knowing how much to stimulate triceps while the subjects activated their remaining muscles during the training period. The synergistic controller showed benefits compared to previous methods for FES controlled elbow extension. It increased the range of forces a subject could generate. Compared to constant stimulation, synergistic control only turned stimulation on when a force was generated in a direction that required elbow extension. Additionally, while only trained under static conditions, synergistic control provided benefits during a dynamic overhead reach task.

While synergistic control showed good initial results, several issues may be explored before implementation in a practical take home system. First, we need to determine whether a single network controller can be trained to operate effectively over all arm geometries and endpoint locations in a subject's workspace. A related issue is the number and selection of muscle inputs required for each controller. It would be useful if we could minimize and easily select which muscles should be implanted with chronic EMG electrodes before surgery. A larger study that included multiple subjects with similar remaining voluntary muscle sets may be able to determine muscle inputs that work best for specific subsets of the C5/C6 SCI population.

In this initial feasibility study, the synergistic controller was trained under static conditions. However, in many real world applications, the controller will operate under dynamic conditions. The lone exception to static testing in our study was overhead reach. While the subject could only complete this task with active elbow extension provided by synergistic control or constant stimulation, the task took twice as long using synergistic control. The increase may be due to the fact that the statically trained controller output is not stable enough under dynamic conditions. Therefore, the initial synergistic controller may be improved by adding a dynamic network structure and dynamic training data.

Finally, continued development of synergistic algorithms that integrate remaining voluntary control with upper extremity neuroprosthetics should not only focus on elbow extension in SCI, but also on restoring shoulder, forearm, and hand function. Adding more degrees of freedom to the SCI upper extremity with FES of paralyzed muscles should increase functionality.